Journal of chemical & engineering data

pubs.acs.org/jced Article

Comparative Study of Influence of Ethanol and 2,2,2-Trifluoroethanol on Thermophysical Properties of 1-Ethyl-3-methylimidazolium Dicyanamide in Binary Mixtures: Experimental and MD Simulations

Urooj Fatima, Riyazuddeen,* Pratik Dhakal, and Jindal K. Shah*

Cite This: https://dx.doi.org/10.1021/acs.jced.0c00447 Read Online

ACCESS | Metrics & More | Article Recommendations | Supporting Information

ABSTRACT: This work focuses on studying the influence exerted on several thermophysical properties of an ionic liquid (IL), 1-ethyl-3-methylimidazolium dicyanamide ([EMIM][DCA]) by alcoholic solvents, ethanol and 2,2,2-trifluoroethanol (TFE), experimentally and computationally. Herein, the densities, ρ, speeds of sounds, u, and dynamic viscosities, η, of the pure IL, [EMIM][DCA]; molecular solvents, ethanol and TFE; and their binary mixtures have been measured over the entire mole fraction ranges at various temperatures from 298.15 to 323.15 K, with an interval of 5 K and at pressure P = 0.1 MPa. The obtained experimental data are utilized to determine the excess/deviation properties, viz., the excess molar volumes, V^E, isentropic compressibility deviations, ΔK_s, and viscosity deviations, $\Delta\eta$. The excess/deviation properties of the studied binary mixtures are fitted to polynomial equations of Redlich−Kister type. The dependence of computed parameters on the composition and temperature and the nature of studied systems is discussed in terms of ion−ion, ion−dipole, hydrogen-bonding, and dipole−dipole interactions. The excess molar volumes of each binary system have been correlated with Prigogine−Flory−Patterson theory. To obtain a molecular-level understanding of the interactions between the IL and cosolvent, molecular dynamics (MD) simulations are employed for two different systems as a function of composition at two different temperatures. Along with thermophysical properties such as density and excess molar volume, the self-diffusion coefficient, radial distribution function, and coordination number are also obtained from MD to provide further insights into fluorine-substituted ethanol (TFE) with IL in order to understand the effect of substitution of fluorine in ethanol in the IL + solvent binary and ternary systems.

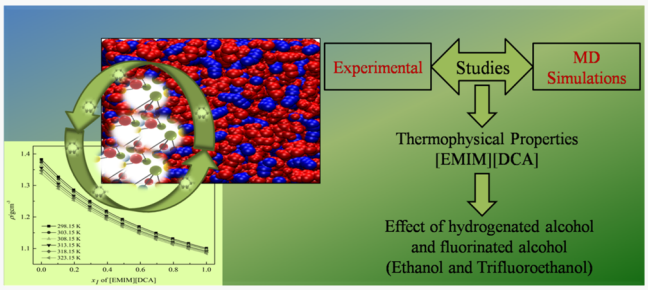

1. INTRODUCTION

Organic salts that are liquids near room temperature are termed ionic liquids (ILs), and they are often called "room-temperature ILs" (RTILs). An ideal amalgamation of cations having low symmetry (imidazolium, ammonium, pyridinium, etc.) with small-sized anions (dicyanamide, halide, trifluoromethane sulfonate, etc.) and weak coordination leads to a complex morphology of ILs.[1] These salts are the greener substitution of volatile organic compounds because of their "distinctive" properties such as the low-melting point, negligible vapor pressure, nonvolatility, high thermal and electrochemical stability, recyclability,[2] the stability of the liquid state over a wide temperature range (around 300 °C), nonflammability, and solubility in a large number of organic solvents.[3] ILs can be widely used as/in biocatalysts, novel solvents for organic/inorganic synthesis, catalysts, synthesis for nanomaterials,[4] extraction processes, aqueous biphasic systems,[5] extractive distillations; solvents for catalytic reactions; and solar cells, heat-transfer fluid,[6] and chemical sensors.[7] Nowadays, a new application of ILs is emerging, that is, for the dissolution of wood components (cellulose, hemicelluloses, and lignin) as these components are insoluble in common solvents which troubled the development of efficient methods for their utilization and analysis. In the wood industry, the commonly employed ILs are imidazolium-based ILs for the treatment of wood and its derivatives.[8] ILs also exhibit a few characteristic features; they show the potential to form hydrogen bonds and to mediate hydrocarbon−solvent interactions.[9] The emphasis on the thermophysical properties of ILs has been upstaged because of their modular nature, that is, the structural modification can be made by altering either

Received: May 12, 2020
Accepted: October 22, 2020

Table 1. Compounds Used with Their CAS Number, Molar Mass, Source, Purification Method, Mass Fraction Purity, and Water Content

compound	CAS number	M/g·mol^{-1}	source	purification method	mass fraction purity (%)[a]	water content
[EMIM][DCA][b]	370865-89-7	177.21	Sigma-Aldrich	Without further purification	≥98	0.014% (Karl Fischer)
TFE[c]	75-89-8	100.04	TCI	Without further purification	≥99	≤0.01%
ethanol	64-17-5	46.07	Merck	Without further purification	≥99	≤0.01%

[a]Purity as stated by the supplier. [b]1-Ethyl-3-methylimidazolium dicyanamide. [c]2,2,2-Trifluoroethanol.

the cation or anion responsible for innumerable combinations, which are feasible and may provide a wide range of ILs as per the required application. Therefore, they are also named "designer solvents" which lead to remarkable progress in various areas of science and industry.[1] For expanding the applications of ILs, the knowledge of physicochemical properties of pure ILs and their binary/ternary mixtures is essential. However, overwhelming amount of literature is available on the binary mixtures of ILs, but details about the thermophysical properties of ternary IL mixtures[10] which contribute significantly toward understanding the nature of intermolecular interactions are scarce. In order to understand the structure−property relationship of IL mixtures that alters upon mixing and exhibits the dependence on the composition and temperature, the thermophysical properties of ILs and polar/apolar solvent mixtures have been investigated through experimental and computational studies. The scientific contribution to the literature of ILs and water mixtures is substantial; however, the studies of IL mixtures with alcoholic moieties are still scarce.[3] Our objective is to generate systematic data on the thermophysical properties of pure RTILs and their binary and ternary mixtures. These experimental studies are indispensable for validating with molecular dynamics (MD) simulations to understand the nature of interaction in ILs and their mixtures which help to predict the thermophysical properties of new systems or to synthesize new ILs. To realize this idea, we have launched the systematic investigation of thermodynamic and transport properties of ILs. 1-Alkyl-3-alkylimidazolium ILs are widely studied presumably due to their easy preparation, nature of stability, flexible and designable ionic structure, comparatively high conductivity, and low-melting point. They are highly miscible in low viscous aprotic organic solvents.[11]

The thermophysical properties are also derived from the fundamental data of density, speed of sound, and dynamic viscosity. The speed of sound is an important thermodynamic property for liquids because of its close relation with compressibility. The transport property and viscosity (for momentum transfer) play an essential role in various chemical and engineering processes. ILs possess relatively high viscosity which is a severe limitation for the application of ILs and necessitates the study of this transport property.

Imidazolium-based ILs provide promising applications in various fields and are considered to be comparatively more versatile. 1-Ethyl-3-methylimidazolium dicyanamide ([EMIM][DCA]) is hydrophilic in nature, and because of this, it imparts excellent ability for accepting hydrogen bonding. The cyano-based anion introduces a great model of water-loving ILs with appealing technological properties. This IL shows comparatively low viscosity (0.02−0.074) Pa·s, and thus, it has potential to be used as a heat-transfer fluid.[12] Our aim is to provide detailed and systematic information on the thermophysical properties of binary mixtures, [EMIM][DCA] + TFE/ethanol. We have opted 2,2,2-trifluoroethanol (TFE) and ethanol as molecular solvents; TFE is opted because of its vast applications. Fluorinated alcohols have revealing unique properties and high technological values in numerous fields of chemical industry, pharmaceuticals, engineering (for instance, as a component in absorption device), and bioengineering.[13] As a solvent, it shows distinctive properties owing to three fluorine atoms which contribute toward weak hydrogen bonding; they are thermally stable above 320 °C and also show a high ionization constant. TFE can induce conformational changes in protein and peptide structures to analyze the structural features of the partially folded state as a cosolvent. It also plays a significant role toward the environment as it is a chlorofluorocarbon substituent as a refrigerant, which destroys the ozone layer. While ethanol is extensively used as a solvent in the manufacturing of varnishes and perfumes, as a preservative for biological specimens; in the preparation of essences and flavors; in many medicines and drugs; as a disinfectant and in tinctures (e.g., tincture of iodine); and as a fuel and gasoline additive.

In this study, we have measured the density (ρ), speed of sound (u), and viscosity (η) of pure [EMIM][DCA], TFE and ethanol, and their binary mixtures, [EMIM][DCA] + TFE, [EMIM][DCA] + ethanol, and TFE + ethanol, in order to understand the effect of ethanol and fluorine-substituted ethanol upon interaction and change in structural conformation in mixtures. Furthermore, from these fundamental data, the temperature-dependent excess/derived properties are also studied that include excess molar volumes, isentropic compressibility deviations, and viscosity deviations, and all the studies are carried out at temperatures T = (298.15, 303.15, 308.15, 313.15, 318.15, and 323.15) K and at atmospheric pressure P = 0.1 MPa. The excess/derived properties are corrected with the Redlich−Kister polynomial equation. The Prigogine−Flory−Patterson (PFP) theory[14−16] is applied for the correlation of V^E of binary mixtures. The hydrogen bond and electrostatic interactions are specifically excluded in this theory and the molecules are considered to be made up of equal segments (isometric portions) in which each segment is capable of interacting with the neighboring site, as every segment has an intermolecular contact site.[15] The PFP theory includes three contributions: (a) an interactional contribution, $V^E_{(int)}$, which is proportional to the only interaction parameter, χ_{21}, (b) free volume, $V^E_{(fv)}$, and (c) internal pressure, $V^E_{(ip)}$.

In addition to this, MD simulations have been performed for the binary mixtures, [EMIM][DCA] + TFE and [EMIM][DCA] + ethanol, as a function of composition at 298.15 and 323.15 K. The computational study supports and interprets the experimental findings along with providing valuable insights into the molecular interactions between the IL and the cosolvents. The studied systems are particularly interesting because [EMIM][DCA] is known to possess low viscosity, while TFE is an acidic alcohol with very little hydrogen-accepting ability. The corresponding densities, self-diffusion

https://dx.doi.org/10.1021/acs.jced.0c00447
J. Chem. Eng. Data XXXX, XXX, XXX−XXX

constants, site−site radial distribution functions (RDFs), and coordination numbers for the hydrogen-bonding interaction for both the mixtures are calculated using MD simulations.

2. EXPERIMENTAL PROCEDURE

2.1. Materials. [EMIM][DCA] (IL), TFE, and ethanol employed in the studies were supplied by Sigma-Aldrich, TCI, and Merck, respectively, and further information about the chemicals is summarized in Table 1. The 3D structures of the pure IL, [EMIM][DCA], and solvents, TFE and ethanol, are represented in Figure 1. However, Figure S1 of the Supporting Information represents the chemical structure of the same. IL and solvents had a low level of water quantity and they were analyzed using a Karl Fischer coulometric titrator (C20, Mettler Toledo) with an electronic digital balance. No additional purifications of the studied compound were performed. A comparison between the experimental density, speed of sound, and viscosity values determined in the present study and those reported in the literature[17−36] is made for the pure IL and solvents at 298.15 K and is presented in Table S1 and graphically represented in Figure 2. A few literature reports are available on [EMIM][DCA]; however, it can be observed that the experimental data on the properties of IL and molecular solvents agree well with the values reported in the literature. The percent deviations (PDs) ([[100·[(Y_{lit} − Y_{exp})/Y_{lit}]] (Y = ρ, u, and η)) for ρ in the case of [EMIM][DCA], TFE, and ethanol are found to be −0.01 to −0.77, 0.06 to −0.08, and 0.07 to −0.31%, respectively. Similarly, the PDs for u for TFE and ethanol are observed in the range of 0.72 to −0.15 and 0.04%, respectively. The PDs observed for η lie in the range of −9.72 to −12.15% for the IL; 0.88 to −3.80% for TFE; and 2.59 to 0.73% for ethanol. The larger deviations observed for dynamic viscosity is due to the fact that we have employed the Anton Paar Lovis 2000 M falling ball automated viscometer, while other authors have determined the viscosity using an ordinary Ubbelohde viscometer and a PC-controlled viscometer Laude iVisc with an Ubbelohde capillary. It can be anticipated that the divergence of our values from those reported in the literature for ρ, u, and η of IL and solvents may be due to the presence of impurities in compounds such as the amount of water in them or due to the use of different experimental methods. Impurities in IL may drastically affect its thermophysical properties.

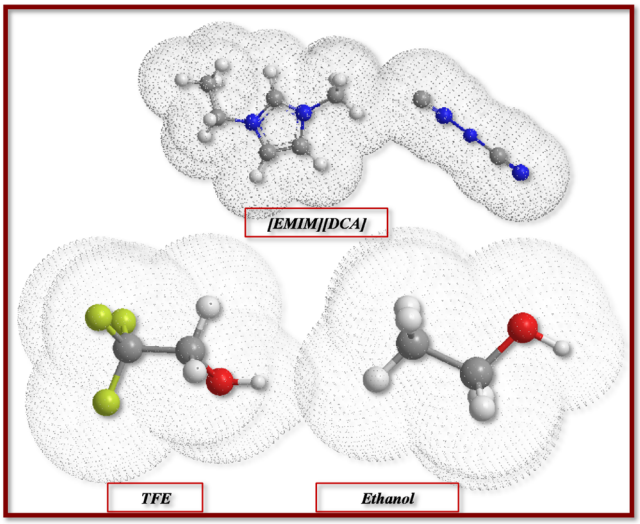

Figure 1. 3D structures of pure [EMIM][DCA], TFE, and ethanol.

2.2. Sample Preparation. Binary mixtures of IL and alcoholic moieties [EMIM][DCA] + TFE, [EMIM][DCA] + ethanol, and TFE + ethanol were prepared on a mass scale, employing a high-precision new classic MS Mettler Toledo electronic digital balance with an uncertainty of 1×10^{-4} g. The estimated combined expanded uncertainty in mole fraction compositions was found to be less than 2×10^{-4}. All samples were freshly prepared before the measurements to avoid variation in the sample composition because of the evaporation of the solution and kept at a desired temperature for some time to ensure the complete miscibility of the sample.

2.3. Density and Speed of Sound Measurements. The densities and speeds of sound of pure components and the homogeneous mixtures of IL with solvents were determined experimentally in the temperature range of 298.15−323.15 K with an interval of 5 K over the entire concentration range and at pressure P = 0.1 MPa with an Anton Paar DSA 5000 M vibrating tube densimeter equipped with an oscillating U-tube sample cell and having a transducer frequency of 3 MHz. The instrument was automatically corrected for the effect of viscosity on the density and speed of sound. The instrument was calibrated for a set of each series of experiments with triply distilled deionized water and dry air. The bubble-free homogeneous sample was injected via a syringe into the U-tube of the instrument. The estimated combined expanded uncertainties with a level of confidence of0.95 and k = 2 associated with the measurements of density and speed of sound were found to be 5×10^{-4} g·cm^{-3} and 0.5 m·s^{-1}, respectively.

2.4. Dynamic Viscosity Measurements. The dynamic viscosities of the studied binary mixtures and their pure components were measured using an Anton Paar Lovis 2000 M falling ball automated viscometer in the temperature range of 298.15−323.15 K with the difference of 5 K over the entire composition range and at atmospheric pressure P = 0.1 MPa. For the determination of viscosities, the instrument having glass capillaries with a diameter of 1.59 mm (dynamic viscosity range = 1−20 mPa·s) and 1.8 mm (dynamic viscosity range = 17−300 mPa·s) was used. The standards N-7.5 and N-26 with standard balls were used to calibrate the capillaries before measurements at temperatures T = 298.15, 303.15, 308.15, 313.15, 318.15, and 323.15 K and at pressure 0.1 MPa. The bubble-free sample was introduced into the capillary of the instrument. The combined expanded uncertainties with a level of confidence of 0.95 and k = 2 associated with measurements of viscosities have been found to be Uc(η) (<1 mPa·s) = 0.20 mPa·s, Uc(η) (1−10 mPa·s) = 0.60 mPa·s, and Uc(η) (11−50 mPa·s) = 0.80 mPa·s. The temperature was kept constant with a precision of 0.01 K.

2.5. MD Simulations. The all-atom optimized potentials for liquid simulations (OPLS-AA) force field was used to model all the three studied systems. The force field parameters for [EMIM][DCA] were taken from the literature,[37,38] while the force field parameters for ethanol and TFE were obtained experimentally.[39] The TFE parameters were on the basis of an earlier study[40] that showed that the OPLS force field for TFE performed best in terms of predicting the diffusion constant, dielectric constant, and thermal expansion coefficient, whereas density estimates were slightly lower compared to other popular TFE force fields. All the force field data used in this

https://dx.doi.org/10.1021/acs.jced.0c00447
J. Chem. Eng. Data XXXX, XXX, XXX−XXX

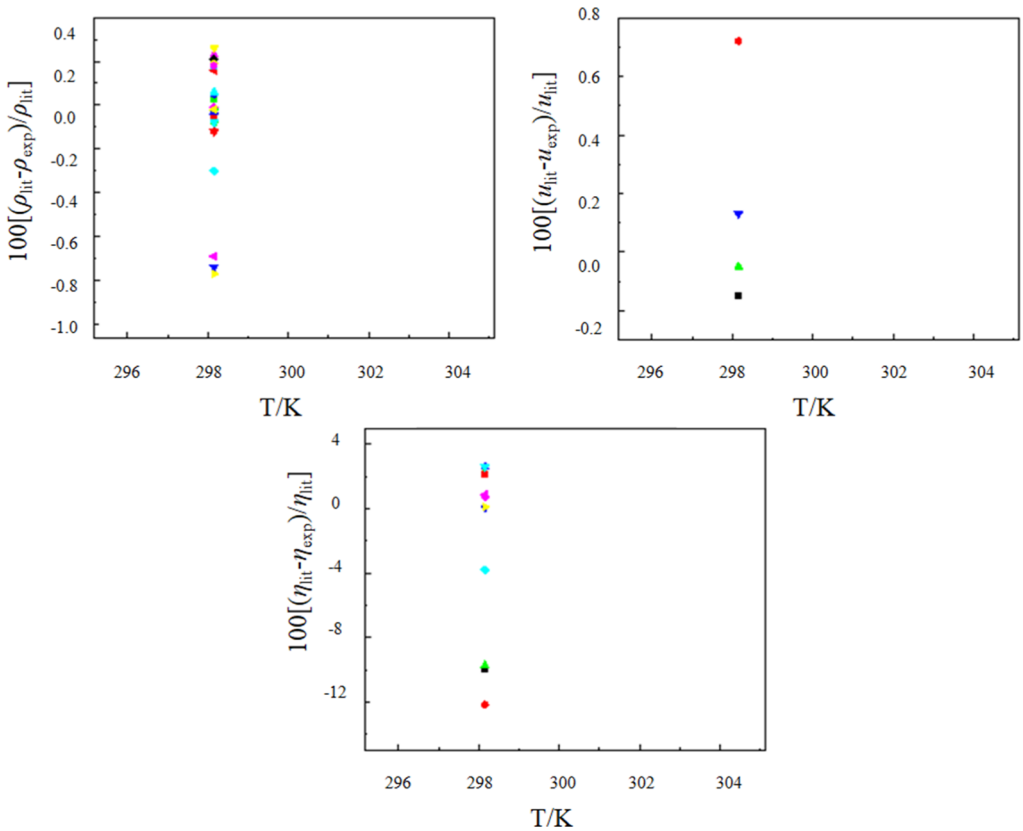

Figure 2. Relative PD $\{100\cdot[(Y_{lit} - Y_{expt})/Y_{lit}]$ ($Y = \rho$, u, and η)$\}$ at T = 298.15 K of experimental values of pure components with the literature (a) ρ for [EMIM][DCA]: solid ■, ref 17; red ●, ref 18; green ▲, ref 19; blue ▼, ref 20; light blue ♦, ref 21; pink ◀, ref 22; yellow ▶, ref 23; ρ for TFE: red ■, ref 24; green ●, ref 25; blue ▲, ref 26; light blue ▼, ref 27; pink ♦, ref 28; light blue ◀, ref 29; green ■, ref 30; blue ●, ref 31; and light blue ▲, ref 32; ρ for ethanol: pink ▲, ref 18; yellow ▼, ref 25; blue ♦, ref 30; red ◀, ref 31; red ▼, ref 32; light blue ■, ref 33, yellow ●, ref 34; pink ●, ref 35; and ♦, ref 36; (b) u for TFE: ■, ref 24; red ●, ref 28; and green ▲, ref 33; u for ethanol: blue ▼, ref 34; (c) η for [EMIM][DCA]: ■, ref 17; red ●, ref 18; and green ▲, ref 19; η for TFE: blue ▼, ref 26; light blue ♦, ref 27; pink ◀, ref 28, and yellow ▶, ref 31; η for ethanol: red ■, ref 18; pink ♦, ref 31; green ●, ref 34; blue ▲, ref 36; and light blue ▼, ref 36.

simulation, along with the functional form of the total potential energy, are provided in the Supporting Information.

MD simulations were performed for pure TFE, ethanol, [EMIM][DCA], and binary mixtures, TFE + [EMIM][DCA] and [EMIM][DCA] +ethanol at various mole fractions (0, 0.050, 0.142, 0.250, 0.333, 0.500, 0.600, 0.822, 0.900, 1.000) and at two different temperatures (298.15 and 323.15 K) using Gromacs 2018.[41] The number of molecules for the TFE and [EMIM][DCA] mixture in the simulation box varied from 256 to 512, as shown in the Supporting Information. The lengths of the simulation box for pure TFE and [EMIM][DCA] were estimated from the experimental densities, while the box lengths for the binary mixtures were calculated assuming an ideal mixing behavior. Figure S2 of the Supporting Information presents the snapshot of the simulation box for [EMIM]-[DCA], while Figures S3−S8 represent the snapshots of interaction between the solvent and the IL. Initial configurations of the studied systems were generated using Packmol.[42]

The MD protocol we adopted involved five steps: the first four steps consisted of minimization of the initial configurations, annealing to the desired temperature, and equilibration in the canonical (*NVT*) and isothermal−isobaric (*NPT*) ensembles, which was followed by an *NPT*-production step. Each of the systems was first minimized using the steepest descent algorithm for 1000 steps. After minimization, the pure IL system and its binary mixtures were subjected to annealing for 1.5 ns. The temperature of each system was raised from 0 K to 298.15 and 323.15 K in linear time steps, held constant at that temperature for 200 ps, and then increased an additional 200 K (498.15 and 523.15 K) in 200 ps. The system temperature was then held constant at 498.15 and 523.15 K for 100 ps after which it was linearly decreased to the reference temperature and finally allowed to stay constant at the reference temperature. All the pure IL systems and their binary mixtures were then equilibrated in *NVT* simulations for 10 ns, followed by 10 ns of the *NPT* ensemble. Finally, the production run lasted for 30 ns in which the Nosé−Hoover thermostat[43] and the Parrinello−Rahman barostat[44] were activated with coupling constants of 0.4 and 2.0 ps, respectively. Data were collected from the last 20 ns of the production run.

During the course of a simulation, hydrogen atoms bonded to heavy atoms have been constrained using the LINCS algorithm. Both Lennard-Jones (LJ) and electrostatic interactions were truncated at 16 Å and the long-range interactions were handled using particle mesh Ewald (PME) summations for LJ and electrostatics with a PME order of 4 and a Fourier spacing of 0.1 nm. Long-range corrections were applied for energy and pressure. Densities obtained for pure [EMIM]-[DCA], ethanol, and TFE from the simulation are in excellent agreement with experimental results with all deviations being less than 2%. The results are provided in Table S2 of the Supporting Information.

https://dx.doi.org/10.1021/acs.jced.0c00447
J. Chem. Eng. Data XXXX, XXX, XXX−XXX

3. RESULTS AND DISCUSSION

3.1. Thermophysical Properties of Binary Systems. In order to understand about the interaction profile between the IL and alcohol-based polar solvents, the densities (ρ), speeds of sound (u), and viscosities (η) were measured over the entire range of mole fractions at six temperatures T = 298.15−323.15 K with the variation of 5 K under atmospheric pressure P = 0.1 MPa. In this study, we have chosen an imidazolium IL, [EMIM][DCA], and polar solvents, TFE and ethanol. Interestingly, TFE is the fluorinated molecule, while ethanol is a hydrogenated molecule of alcohol, and both are associated via hydrogen bonding. Herein, our concern is to understand the difference in the effect of fluorinated alcohol, TFE, and hydrogenated alcohol, ethanol, on the imidazolium IL in binary mixtures. The measured ρ, u, and η values of IL with polar solvents are presented as a function of IL concentration and temperature in Tables S3−S5 of the Supporting Information for all the three studied binary systems.

The density data of binary mixtures obtained from MD simulations are found to be in excellent agreement with experimental results in both studied mixtures. Using a spline interpolation, the simulated densities are interpolated at the required experimental mole fractions with root-mean-square deviations and found to be 0.011 and 0.012 g/cm^3 for the [EMIM][DCA] + TFE mixture while 0.010 and 0.011 g/cm^3 for [EMIM][DCA] + ethanol at 298.15 and 323.15 K, respectively. The comparison plots for experimental and simulated ρ at 298.15 and 323.15 K for the [EMIM][DCA] + TFE/ethanol system are depicted in Figures S9 and S10 (Supporting Information). The ρ values of IL + TFE do not follow a similar and usual trend as shown by IL + ethanol. The ρ values for the mixture of IL + TFE show a slightly decreasing trend with increasing concentration at all studied temperatures, while the IL + ethanol binary system reveals an increase in ρ values with concentration, and the values decrease with temperature for both systems. The factor responsible for the unusual trend [EMIM][DCA] + TFE may be due to the presence of the F atom in the alcohol moiety instead of the H atom, as F is a highly electronegative atom. As discussed above, the ρ values increase with increasing mole fraction of IL for the [EMIM][DCA] + ethanol system, suggesting that the effects of TFE and ethanol on the IL were opposite. In order to understand the nature of the IL−solvent system in-depth, we concentrated on the solvent system and for that we included the study of the TFE + ethanol mixture in this work. The effect of mixing a fluorinated alcohol with a hydrogenated alcohol is presented as a straight-line plot of ρ with a usual trend; this may be due to the compensation effect of TFE and ethanol in the binary mixture. The measured values of densities are depicted in Table S2 of the Supporting Information.

Quijada-Maldonado et al.[18] reported the ρ value at 298.15 K for the binary system, [EMIM][DCA] + ethanol, as 0.869589 at x_1 = 0.0997, while at the same mole fraction, our value was 0.875651 and the PD was 0.697%. Some authors[25,30,32] have also reported the density data at 298.15 K for the binary mixture, ethanol + TFE. Our value of ρ in this work at x_1 = 0.1081 was found to be 0.858366 g·cm^{-3}, however, at the same mole fraction, Minamihonoki et al.[25] reported it as 0.857266 g·cm^{-3} with a PD of 0.13%. Sassi and Atik.[30] and Duarte et al.[32] reported the ρ values as 0.858893 and 0.857138 g·cm^{-3} with PDs of 0.06% and 0.143%, respectively, at the same mole fraction. The literature data at the given mole fractions were obtained by extrapolation. The inconsiderable deviation in the values may be ascribed to certain undefined impurities in compounds or to the use of different experimental methods.

Furthermore, the values of speed of sound for IL and TFE/ethanol mixtures over the whole range of composition at all studied temperatures and at P = 0.1 MPa have also been measured experimentally. The measured value of u is found to be increased with the mole fraction of IL for the [EMIM]-[DCA] + TFE and [EMIM][DCA] + ethanol systems, while for the system containing fluorinated and hydrogenated alcohols, TFE + ethanol, the values of u show a reverse trend, that is, decreasing behavior with increasing mole fraction of TFE. The temperature dependence of u shows a decreasing effect with an increase in temperature for all the three concerned systems. The values of [EMIM][DCA] + TFE, [EMIM][DCA] + ethanol systems, and TFE + ethanol mixtures are listed in Table S4 of the Supporting Information.

The mixture of an IL with a less viscous solvent reveals great industrial applications, especially in the battery industry. In this work, to overcome the hindrance of viscous IL in industries, we have also studied the viscosity of the pure IL and its binary/ternary mixtures. It is evident from Table S5 (Supporting Information) that η values increase with IL mole fraction and decrease with temperature for all the studied binary mixtures. This trend may be ascribed to the strong interaction between the ion strengthening upon mixing with polar molecular solvents and to the hydrogen bonding. Quijada-Maldonado et al.[18] reported the value of η for [EMIM][DCA] + ethanol at T = 298.15 K and at the mole fraction x_1 = 0.0997 as 1.74 m·s^{-1}, while our value is found to be 1.85 m·s^{-1}. The literature value at the same mole fraction is obtained by intrapolation and the PD is −5.945%. Such a large PD observed for dynamic viscosity is due to different instruments employed.

The experimental data of ρ, u, and η are employed to determine the derived/excess properties. We have obtained excess molar volumes (V^E), isentropic compressibility deviations (ΔK_s), and viscosity deviations ($\Delta\eta$) for all binary mixtures focused in this work. The V^E, ΔK_s, and $\Delta\eta$ of the imidazolium IL with fluorinated and hydrogenated alcohols as a function of mole fraction of IL/TFE at all the concerned six temperatures under P = 0.1 MPa are presented in Tables S6, S8, and S9 of the Supporting Information, respectively. Eventually, the composition-dependent V^E, ΔK_s, and $\Delta\eta$ provide information about the nature of interaction between ions of IL and polar solvent molecules and also help to explain the interactions in the solvent−solvent mixture. The calculated parameters are correlated by means of the following Redlich−Kister polynomial equation

$$Y^E = x_1(1 - x_1)\frac{\sum_{i=0}^{m} A_i(2x_1 - 1)^i}{1 + \sum_{j=1}^{n} B_j(2x_1 - 1)^j} \quad (1)$$

$$\sigma(Y^E) = \left[\sum_{i=1}^{p} \frac{(Y^E_{cal} - Y^E_{exp})^2}{(p - (m + n + 1))}\right]^{1/2} \quad (2)$$

where Y^E refers to the V^E or ΔK_s or $\Delta\eta$; m and n are the degrees of polynomial; A_i and B_j are adjustable parameters; and x_1 is the mole fraction of [EMIM][DCA]/TFE. The adjustable parameters A_i and B_j have been obtained by fitting eq 1 to the experimental data using a least-squares regression method. In each case, the optimum numbers of coefficients are ascertained from an examination of standard deviation (σ) values. The

https://dx.doi.org/10.1021/acs.jced.0c00447
J. Chem. Eng. Data XXXX, XXX, XXX−XXX

Table 2. Coefficients of Eq 2 for Excess Molar Volumes, V^E(m^3·mol^{-1}), Isentropic Compressibility Deviations, ΔK_s (10^{-10}/(m^2·N^{-1})), Viscosity Deviations, $\Delta\eta$ (mPa·s), and Standard Deviations, σ, at Temperature T = 298.15−323.15 K and Mole Fraction, x_1, for [EMIM][DCA] + TFE, [EMIM][DCA] + Ethanol, and TFE + Ethanol Systems at Pressure P = 0.1 MPa

	T/K	A_0	A_1	A_2	A_3	B_1	σ
			[EMIM][DCA] + TFE				
V^E	298.15	−0.9221	−0.6464	−0.1712		0.7484	0.0025
	303.15	−0.9521	−0.5585	−0.2475		0.6388	0.0027
	308.15	−0.9813	−0.3589	−0.4475		0.4127	0.0050
	313.15	−1.0075	−0.0853	−0.6474		0.1743	0.0076
	318.15	−1.0473	0.0895	−0.8077		0.0417	0.0098
	323.15	−1.0895	−0.0714	−0.8463		0.1620	0.0109
			[EMIM][DCA] + Ethanol				
V^E	298.15	−5.4400	4.8672	−3.9305		0.1581	0.0048
	303.15	−5.5471	5.1850	−4.4258		0.1118	0.0064
	308.15	−5.6010	5.4002	−4.8917		0.0765	0.0122
	313.15	−5.6585	5.3411	−5.1556		0.0848	0.0138
	318.15	−5.7555	5.4075	−5.2410		0.0785	0.0159
	323.15	−5.8240	5.7675	−5.7383		0.0340	0.0190
			TFE + Ethanol				
V^E	298.15	3.8916	−4.9172	0.4649		−1.1393	0.0093
	303.15	3.9766	−5.2985	0.5958		−1.2028	0.0116
	308.15	4.0904	−5.6867	0.6697		−1.2633	0.0151
	313.15	4.1717	4.8500	−0.7555		1.2998	0.0174
	318.15	4.2482	4.7215	−0.6868		1.2449	0.0173
	323.15	4.3386	4.5160	−0.5400		1.1636	0.0138
			[EMIM][DCA] + TFE				
ΔK_s	298.15	−10.5158	2.2469	0.5453	4.6275	0.5641	0.0295
	303.15	−11.6994	−1.7879	2.2625	−1.5507	0.8935	0.0107
	308.15	−12.3294	−1.7878	2.2052	−1.4337	0.8841	0.0118
	313.15	−12.9941	−1.5951	1.9322	−1.2284	0.8622	0.0105
	318.15	−13.7354	−1.8389	2.3102	−1.6285	0.8825	0.0140
	323.15	−14.5233	−1.8657	2.3038	−1.5922	0.8775	0.0084
			[EMIM][DCA] + Ethanol				
ΔK_s	298.15	−10.6581	0.4986	−0.0968	−0.0752	0.7293	0.0042
	303.15	−11.1660	0.4418	−0.1229	−0.0393	0.7359	0.0034
	308.15	−11.7144	0.3206	0.0746	−0.2698	0.7542	0.0046
	313.15	−12.2603	0.6363	−0.3409	0.0125	0.7324	0.0054
	318.15	−12.8780	0.7502	−0.4318	0.1829	0.7263	0.0048
	323.15	−13.5163	0.8418	−0.5531	0.2471	0.7252	0.0078
			TFE + Ethanol				
ΔK_s	298.15	3.1044	−1.8428	0.0407	−0.5442	−0.7372	0.0053
	303.15	3.3473	−2.0948	0.0603	−0.5779	−0.7678	0.0057
	308.15	3.6148	−2.0032	0.1079	−0.6723	−0.7024	0.0067
	313.15	3.8925	−2.0141	0.1606	−0.7183	−0.6634	0.0075
	318.15	4.1852	−1.8906	0.2511	−0.8046	−0.5991	0.0085
	323.15	4.8511	−5.8916	0.2476	−1.3155	−1.3319	0.0040
			[EMIM][DCA] + TFE				
$\Delta\eta$	298.15	−1.1198	0.3815	0.0330		−0.6575	0.0035
	303.15	−0.9758	0.7976	0.1307		−1.0303	0.0023
	308.15	−0.8265	0.5983	0.1982		−1.0221	0.0042
	313.15	−0.7121	0.7167	0.2411		−1.2696	0.0031
	318.15	−0.6047	0.5604	0.1577		−1.1711	0.0018
	323.15	−0.5229	−0.8851	−0.2583		1.3251	0.0050
			[EMIM][DCA] + Ethanol				
$\Delta\eta$	298.15	−5.1245	5.1408	2.8699		−0.8074	0.0393
	303.15	−3.9374	4.1179	2.5660		−0.7714	0.0286
	308.15	−2.9842	3.4035	2.0453		−0.7740	0.0239
	313.15	−2.2776	2.7586	1.7636		−0.7700	0.0191
	318.15	−1.7360	2.3000	1.4578		−0.7389	0.0132
	323.15	−1.3405	1.8868	1.3560		−0.7144	0.0105
			TFE + Ethanol				
$\Delta\eta$	298.15	−1.1198	0.3815	0.0330		−0.6575	0.0035
	303.15	−0.9758	0.7976	0.1307		−1.0303	0.0023

https://dx.doi.org/10.1021/acs.jced.0c00447
J. Chem. Eng. Data XXXX, XXX, XXX−XXX

Table 2. continued

T/K	A_0	A_1	A_2	A_3	B_1	σ
			TFE + Ethanol			
308.15	−0.8265	0.5983	0.1982		−1.0221	0.0042
313.15	−0.7121	0.7167	0.2411		−1.2696	0.0031
318.15	−0.6047	0.5604	0.1577		−1.1711	0.0018
323.15	−0.5113	−2.9882	−1.0521		5.4320	0.0045

standard deviation, σ, has been calculated from eq 2. Here, p is the number of experimental data points. The choice of m and n values for the degrees of polynomial in eq 2 was made using Akaike's information criterion.[15] The values of the fitted parameters A_i, B_j are given in Table 2 along with standard deviations.

The V^E behavior reveals the deviations from ideality. The V^E are computed for the binary mixtures, [EMIM][DCA] + TFE/ethanol and TFE + ethanol, using the following equation

$$V^E = \sum_{i=1}^{N} x_i M_i (\rho^{-1} - \rho_i^{-1}) \tag{3}$$

where ρ is the density of the binary mixture; ρ_i is the density of the pure component i; and M_i and x_i represent the molar mass and mole fraction of pure components, respectively.

The obtained excess property, V^E, of the studied binary mixtures of IL with TFE and ethanol is negative over the whole range of concentration at all the focused temperatures with minima at x_1 = 0.5 for IL + TFE and at x_1 = 0.3 for IL + ethanol systems. The deviation becomes more negative with increasing temperature from 298.15 to 323.15 K for both the binary mixtures, IL + TFE/ethanol. However, for the TFE + ethanol system, the V^E are found to be positive over the entire mole fraction range at all temperatures with minima at x_1 = 0.9. With increasing temperature from 298.15 to 323.15 K, the magnitude of excess molar volume becomes more positive. The table and plots of V^E at all temperatures are shown in Table S6 (Supporting Information) and Figure 3a−c. The negative deviation from ideality for the binary systems IL + TFE/ethanol is also substantiated by simulation studies and reported in Table S7 and Figures S11 and S12 (Supporting Information). As observed from Figure S11 (Supporting Information), the simulation study captures the consistent sign of deviation and temperature dependency to the experimental results for [EMIM][DCA] + TFE but overestimates the negative deviation. The simulation data of V^E for [EMIM][DCA] + ethanol are in good agreement with experimental data, as observed from Figure S12 (Supporting Information). This difference in deviation from experimental data between Figures S11 and S12 (Supporting Information) could be due to underpredicting the density of pure TFE with the OPLS-AA force field as we mentioned earlier, and second, V^E values are extremely sensitive to slight changes in density values. The negative deviation from ideality indicates the presence of a more attractive interaction in the mixture than in the pure components, and it elucidates the attractive interaction occurred, owing to the accommodation of molecules of one component into the interstitial sites of the structural network of the other component. Moreover, it also contributes to the interaction between unlike molecules such as the formation of H-bonds or charge-transfer complexes or any other nonspecific forces (ion−dipole interactions, etc.) resulted in a decrease in volume. Furthermore, the negative deviation also reveals that the system has a stronger packing efficiency via heteroassociation between the ions of ILs and solvents and other nonspecific forces. The interaction between molecules of TFE/ethanol with ions of IL may be ascribed to ion−dipole attractive interactions or other nonspecific forces.

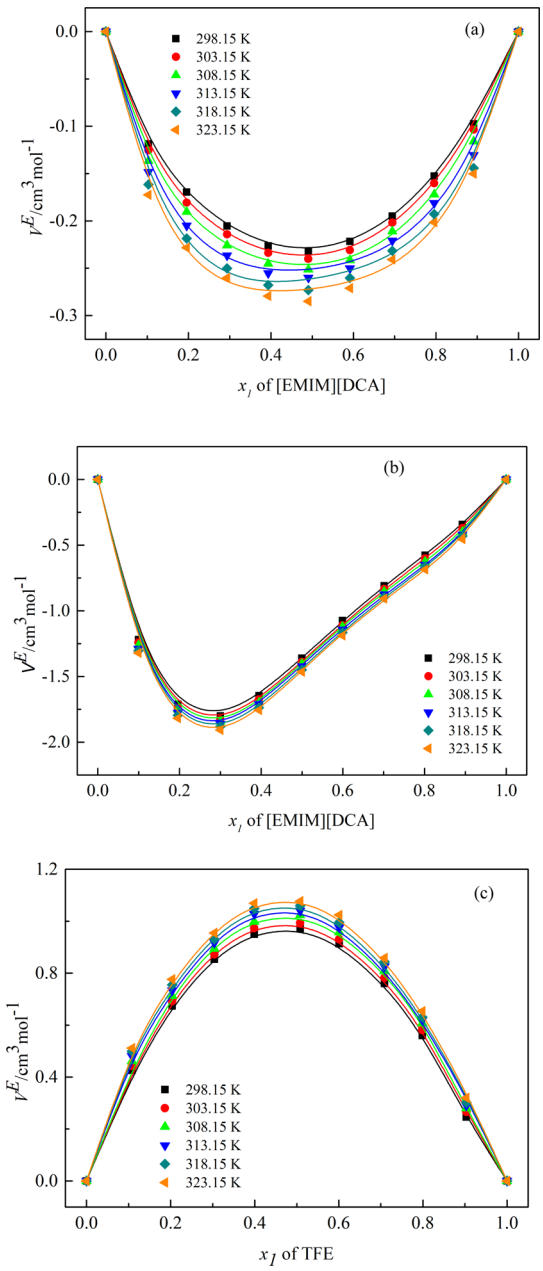

Figure 3. Excess molar volumes (V^E/cm^3 mol^{-1}) of (a) [EMIM][DCA] + TFE, (b) [EMIM][DCA] + ethanol, and (c) TFE + ethanol as a function of mole fraction at different temperatures. The symbols represent experimental values and the solid curves represent calculated values by the Redlich−Kister equation.

https://dx.doi.org/10.1021/acs.jced.0c00447
J. Chem. Eng. Data XXXX, XXX, XXX−XXX

Interestingly, in the IL + ethanol mixture, the magnitude of negative values of V^E is larger compared to the values of the IL + TFE system, as also seen from the simulation results in Figures S11 and S12 (Supporting Information). These results explicitly suggest that ethanol has a strong ability to interact with IL molecules; therefore, more negative values of V^E have been found for the IL and ethanol mixture.

The positive values of V^E are attributed to the existence of nonspecific interactions between molecules in mixtures. However, for the TFE + ethanol system, the positive V^E values may be ascribed to the weaker association between the molecules of TFE and ethanol via H-bonding. The type of interaction is reflected by the magnitude and sign of V^E. It may also be explained in terms of hydrogen bonding. The hydrogen-bonding ability of TFE is lower compared to that of ethanol. Therefore, the less negative value of V^E in IL + TFE may be due to weaker hydrogen bonding association in contrast to that in IL + ethanol. It may also be concluded that the interaction within the similar molecules of solvent is of higher degree as compared to the binary mixture of TFE + ethanol.

The experimental data of density and speed of sound have been employed to calculate the isentropic compressibility values K_s of all the binary mixtures by using the Newton−Laplace equation.

$$K_S = (1/V_m)(\partial V_m/\partial p)_S = 1/\rho(\partial\rho/\partial p)_S = 1/(\rho\cdot u^2) \quad (4)$$

where V_m is the molar volume and K_S is the isentropic compressibility.

The experimental isentropic compressibility deviations (ΔK_s) for the studied binary mixtures, [EMIM][DCA] + TFE/ethanol and TFE + ethanol, have been determined using the following relation

$$\Delta K_s = K_s - \sum_{i=1}^{N} x_i K_{si} \quad (5)$$

where K_s is the isentropic compressibility and K_{si} and x_1, x_2 are isentropic compressibilities and mole fractions of pure components, respectively.

Table S8 of the Supporting Information and Figure 4a−c for ΔK_s suggest that the ΔK_s of the studied systems, [EMIM]-[DCA] + TFE/ethanol, are found to be negative throughout the composition range at all the studied temperatures under atmospheric pressure, while for the TFE + ethanol system, all the values of ΔK_s are found to be positive over the entire mole fraction range. Its values decrease and become more negative with the rise of temperature for the binary mixtures [EMIM][DCA] + TFE and [EMIM][DCA] + ethanol. Furthermore, for the TFE + ethanol binary system, the values increase with temperature. The positive values of isentropic compressibility deviations suggest the existence of weak interaction among the components of the mixture. On the other hand, the negative values reveal the existence of strong interactions between the IL and the solvent molecule and solvent−solvent molecules.

The $\Delta\eta$ for the considered binary mixtures, [EMIM][DCA] + TFE, [EMIM][DCA] + ethanol, and TFE + ethanol, have been evaluated from the viscosity data of pure and binary mixtures using the following expression

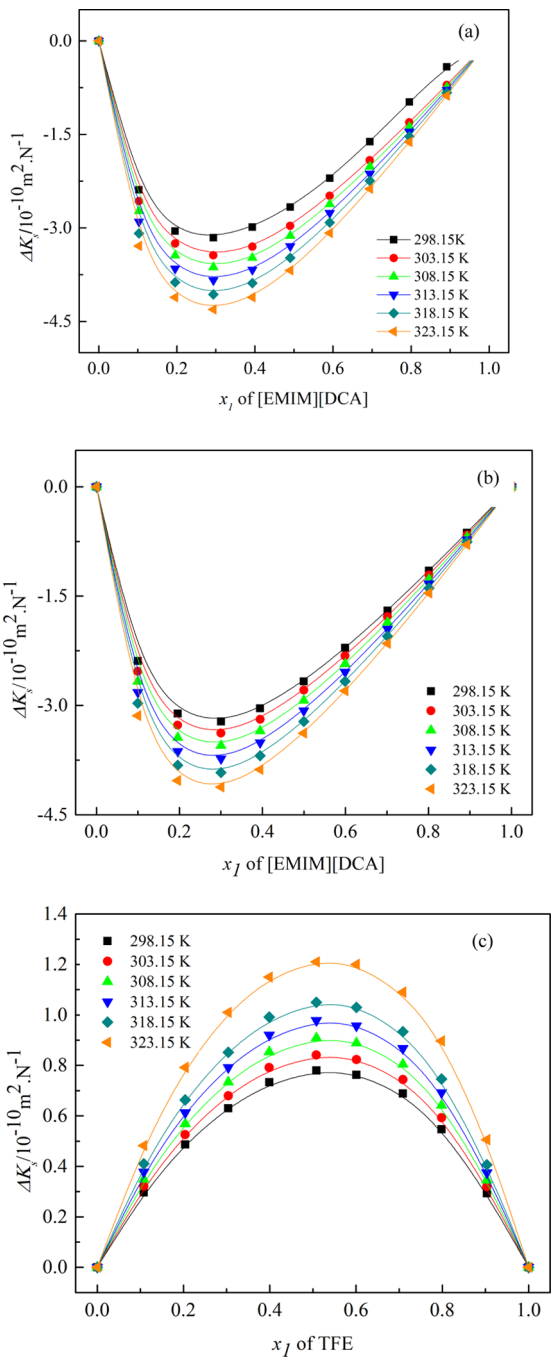

Figure 4. Isentropic compressibility deviations ($\Delta K_s/10^{-10}$ m^2·N^{-1}) of (a) [EMIM][DCA] + TFE, (b) [EMIM][DCA] + ethanol, and (c) TFE + ethanol as a function of mole fraction at different temperatures. The symbols represent experimental values and the solid curves represent calculated values by the Redlich−Kister equation.

$$\Delta\eta = \eta - \sum_{i=1}^{N} x_i\eta_i \quad (6)$$

where η_i and η are the dynamic viscosity of pure component i and binary mixtures, respectively, while x_i is the mole fraction of the pure component i.

The determined values of $\Delta\eta$ for all the investigated systems obtained from eq 6 are depicted in Table S9 (Supporting Information) and Figure 5a−c. An examination of the plots

https://dx.doi.org/10.1021/acs.jced.0c00447
J. Chem. Eng. Data XXXX, XXX, XXX−XXX

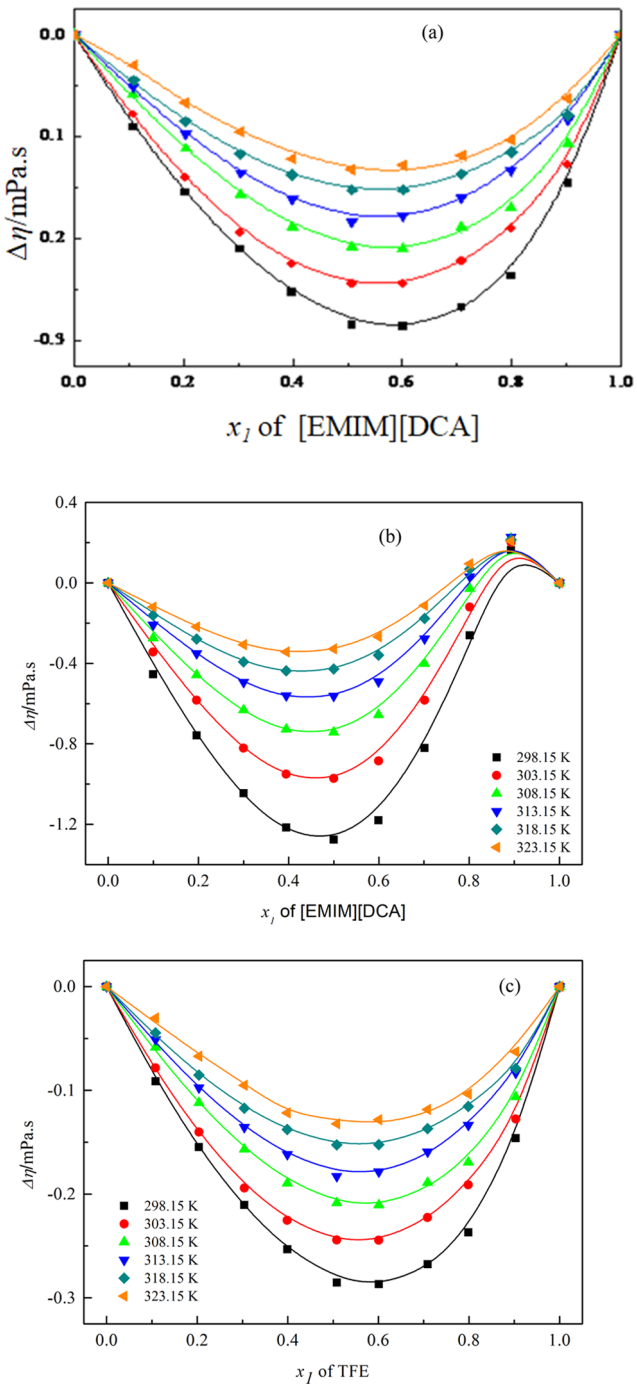

Figure 5. Viscosity deviations ($\Delta\eta$/mPa·s) of (a) [EMIM][DCA] + TFE, (b) [EMIM][DCA] + ethanol, and (c) TFE + ethanol as a function of mole fraction at different temperatures. The symbols represent experimental values and the solid curves represent calculated values by the Redlich−Kister equation.

reveals the negative deviation of $\Delta\eta$ from an ideal mixture for all the concerned binary systems, although the magnitude of the negative deviation is comparatively less in the TFE + ethanol system, whereas there is very slight difference in deviation in the case of [EMIM][DCA] + TFE/ethanol systems. It can be noticed that $\Delta\eta$ is slightly more negative in the case of IL + TFE than that of the IL + ethanol system. Generally, the deviation in viscosity shows their dependence on the size and shape of the molecules as well as on the prevalence of different types of interaction between the components of the mixture. This may also be explained on the basis of optimum accommodation of solvent molecules into the interstitial sites of the molecular structural network of ions of IL. The negative values of $\Delta\eta$ may be attributed toward stronger interaction including ion−dipole, dipole−dipole, and van der Waals forces or hydrogen-bonding interactions. On the basis of this, we can say that the interaction becomes quite weaker in TFE + ethanol in contrast to that in the IL + TFE/ethanol system.

3.2. Application of PFP Theory. The PFP theory[14−16] is applied for the quantitative correlation of V^E of binary mixtures, [EMIM][DCA] + TFE, [EMIM][DCA] + ethanol, and TFE + ethanol at temperatures T = 298.15−323.15 K with the variation of 5 K and under pressure P = 0.1 MPa. In PFP theory, the hydrogen-bonding interactions and electrostatic forces of interactions are specifically excluded. According to the PFP theory, a molecule is considered to be made up of equal segments (isometric portions) in which each segment is capable of interacting with the neighboring site, as every segment is having intermolecular contact sites.[15] In this work, the PFP theory has been applied to analyze and correlate the V^E values in terms of three contributions, (a) an interactional contribution, $V^E_{(int)}$, which is proportional to the only interaction parameter, χ_{21} (b) free volume, $V^E_{(fv)}$, and (c) internal pressure contribution, $V^E_{(ip)}$. The following mathematical expression has been employed to compute the V^E values in this study[14−16]

$$\frac{V^E}{x_1V_1^* + x_2V_2^*} = \frac{V^E_{(int)}}{x_1V_1^* + x_2V_2^*} + \frac{V^E_{(fv)}}{x_1V_1^* + x_2V_2^*} + \frac{V^E_{(ip)}}{x_1V_1^* + x_2V_2^*}$$
$$= \frac{(\tilde{V}^{1/3} - 1)\tilde{V}^{2/3}\Psi_2\theta_1\chi_{21}}{[(4/3)\tilde{V}^{-1/3} - 1]\,P_2^*} + \frac{-(\tilde{V}_1 - \tilde{V}_2)^2((14/9)\tilde{V}^{-1/3} - 1)\Psi_1\Psi_2}{[(4/3)\tilde{V}^{-1/3} - 1]\tilde{V}} + \frac{(\tilde{V}_1 - \tilde{V}_2)(P_1^* - P_2^*)\Psi_1\Psi_2}{P_2^*\Psi_1 + P_1^*\Psi_2} \quad (7)$$

where x_i, V_i^*, V_i, $\bar{V}_i$, ϕ_i, Ψ_i, θ_i, S_i, P_i^*, and $k_{T,i}$ are the mole fraction, characteristic volume, molar volume, reduced volume, hard-core volume fraction, molecular contact energy fraction, molecular surface fraction, molecular surface/volume ratio, characteristic pressure, and the isothermal compressibility of pure components, respectively. $\bar{V}$ is the reduced volume of the mixtures. The values of V_i^*, V_i, $\bar{V}_i$, ϕ_i, Ψ_i, θ_i, S_i, P_i^*, and k_{Ti} are determined using the method reported in our earlier publication.[15] The procedure for the calculation of the isobaric thermal expansion coefficient α_i values of pure components [EMIM][DCA],TFE, and ethanol are also mentioned in our earlier publication.[15] The molar heat capacities, C_p, of [EMIM][DCA] are taken from the literature,[45] while the data of C_p for TFE are calculated from the equation provided by Alberto Coronas et al.[46] The C_p values for ethanol are also obtained from the literature.[47−49]

On least squares fitting of the experimental V^E to eq 7, the interactional parameter χ_{21} data of all studied binary systems have been determined over the entire composition range and

https://dx.doi.org/10.1021/acs.jced.0c00447
J. Chem. Eng. Data XXXX, XXX, XXX−XXX

Table 3. Experimental Excess Molar Volumes, $V^E_{(exp)}$, Correlated Excess Molar Volumes, $V^E_{(PFP)}$, Interactional Parameter, χ_{21}, Internal Energy, $V^E_{(int)}$, Free Volume, $V^E_{(fv)}$, and Internal Pressure, $V^E_{(ip)}$, at Mole Fraction x_1 = 0.5 for [EMIM][DCA] + TFE, at Mole Fraction x_1 = 0.3 [EMIM][DCA] + Ethanol, and at Mole Fraction x_1 = 0.9 for TFE + Ethanol Systems at Different Temperatures and Pressure P = 0.1 MPa

T/K	$V^E_{(expt)}$ cm^3·mol^{-1}	$V^E_{(PFP)}$ cm^3·mol^{-1}	χ_{21} J·cm^{-1}	$V^E_{(int)}$ cm^3·mol^{-1}	$V^E_{(fv)}$ cm^3·mol^{-1}	$V^E_{(ip)}$ cm^3·mol^{-1}
			[EMIM][DCA] + TFE			
298.15	−0.2318	−0.2331	126.00	0.9061	−0.5752	−0.5628
303.15	−0.2400	−0.2810	132.12	0.9620	−0.5964	−0.6054
308.15	−0.2513	−0.3362	137.21	1.0212	−0.6168	−0.6590
313.15	−0.2600	−0.3761	141.11	1.0711	−0.6397	−0.6946
318.15	−0.2731	−0.4301	146.20	1.1300	−0.6503	−0.7563
323.15	−0.2849	−0.5010	153.10	1.2100	−0.6648	−0.8318
			[EMIM][DCA] + Ethanol			
298.15	−1.8011	−1.8012	−119.01	−0.8580	−0.3339	−0.6089
303.15	−1.8289	−1.8600	−115.00	−0.8451	−0.3439	−0.6397
308.15	−1.8446	−1.9211	−108.04	−0.8111	−0.3536	−0.6799
313.15	−1.861	−1.9802	−104.30	−0.7900	−0.3706	−0.7011
318.15	−1.8814	−2.0501	−97.91	−0.7622	−0.3807	−0.7392
323.15	−1.9079	−2.1300	−91.01	−0.7231	−0.3919	−0.7924
			TFE + Ethanol			
298.15	0.2461	0.2460	64.30	0.2391	−0.0052	0.0119
303.15	0.2660	0.2541	67.52	0.2590	−0.0056	0.0123
308.15	0.2798	0.2635	68.41	0.2732	−0.0061	0.0127
313.15	0.2908	0.2709	69.30	0.2854	−0.0062	0.0121
318.15	0.3016	0.2798	69.63	0.2971	−0.0062	0.0114
323.15	0.3199	0.2909	71.00	0.3150	−0.0064	0.0112

at all temperatures. The χ_{21} obtained represents the intermolecular interaction between the components of mixtures, and its values at x_1 = 0.5 for [EMIM][DCA] +TFE, at x_1 = 0.3 for [EMIM][DCA] + ethanol, and at x_1 = 0.9 for TFE + ethanol systems and at temperatures T = 298.15−323.15 K are listed in Table 3. The x_1 = 0.5, 0.3, and 0.9 for [EMIM][DCA] + TFE, [EMIM][DCA] + ethanol, and TFE + ethanol are chosen as minimum values of experimental V^E lying at these mole fractions, respectively. Figure 6a−c exhibits the values of correlated and experimental V^E and the three PFP contribution values at T = 298.15 K for all three studied binary systems over the whole range of compositions. The χ_{21} are found to be positive for the system containing fluorine-substituted alcohol, that is, [EMIM][DCA] +TFE and TFE + ethanol; however, for the [EMIM][DCA] + ethanol system, χ_{21} is found to be negative over the entire concentration range, but for the effect of temperature, it is observed that the value varies from negative to positive. As can be seen in Table 3, the variation of χ_{21} with temperature is positive for the systems, [EMIM][DCA] +TFE and TFE + ethanol. The free-volume contribution, $V^E_{(fv)}$, is found to be negative and its magnitude increases with increasing temperature, which reveals that as the temperature increases, more free volume in the [EMIM][DCA] molecules matrix become available to accommodate the TFE/ethanol molecules in [EMIM][DCA] + TFE, [EMIM][DCA] + ethanol, and to TFE molecules in the TFE + ethanol system. The contribution of $V^E_{(fv)}$ indicates the available free volume/interstitial accommodation space in the system. The characteristic pressure, $V^E_{(ip)}$, which depends on the structure-breaking effect and is proportional to $(P_1^* - P_2^*)$ $(\bar{V}_1 - \bar{V}_2)$ has negative values for the [EMIM][DCA] + TFE and [EMIM][DCA] + ethanol systems and positive values for TFE + ethanol. The variation of values of $V^E_{(ip)}$ corresponds to different degrees of hydrophobic forces operating in the systems. The $V^E_{(int)}$ term represents the energy of interaction and its value is found to be positive for the binary mixtures, [EMIM][DCA] + TFE and TFE + ethanol, whereas such values are found to be negative for the [EMIM][DCA] + ethanol system. The experimental and PFP-correlated values of V^E for the [EMIM][DCA] + TFE system at $x_1 \approx 0.49$ are (−0.2318, −0.2331) cm^3·mol^{-1} with a PD of 0.56%, for the [EMIM][DCA] + ethanol system at $x_1 \approx 0.30$ are (−1.8011, −1.8012) cm^3·mol^{-1} with a PD of 0.01%, and for the TFE + ethanol system at $x_1 \approx 0.90$ are (0.2461, 0.2460) with a PD value of 0.04%. Thus, the experimental and PFP-correlated values of V^E are in good agreement with each other.

3.3. MD Simulations. *3.3.1. Self-Diffusion Constant.* In order to explain the trend of variation of viscosity with composition, we determined the self-diffusion coefficients for the cation and anion of IL in the [EMIM][DCA] + TFE and [EMIM][DCA] + ethanol mixtures at 298.15 and 323.15 K by fitting the linear region of the mean-square-displacement (MSD) values as a function of time over 4−8 ns obtained from MD simulations. The MSD values of cation and anion of pure ILs and their mixtures [EMIM][DCA] + TFE and [EMIM]-[DCA] + ethanol at 298 K over 20 ns are plotted in Figures S13−S15 respectively; however, the linear fitting region of 4−8 ns MSD of pure ILs and their mixtures [EMIM][DCA] + TFE and [EMIM][DCA] + ethanol is plotted in Figures S16−S18 (Supporting Information). The results are reported in Table S10 of the Supporting Information and plotted in Figures S19 and S20 (Supporting Information) for the two mixtures. The self-diffusion constants are computed from MSD data using the Einstein relation employing eq 8

$$D = \frac{1}{6}\lim_{t\to\infty}\frac{\mathrm{d}}{\mathrm{d}t}\left\langle \sum_{i=1}^{N}[\vec{r}_i(t) - \vec{r}_i(0)]^2 \right\rangle \quad (8)$$

https://dx.doi.org/10.1021/acs.jced.0c00447
J. Chem. Eng. Data XXXX, XXX, XXX−XXX

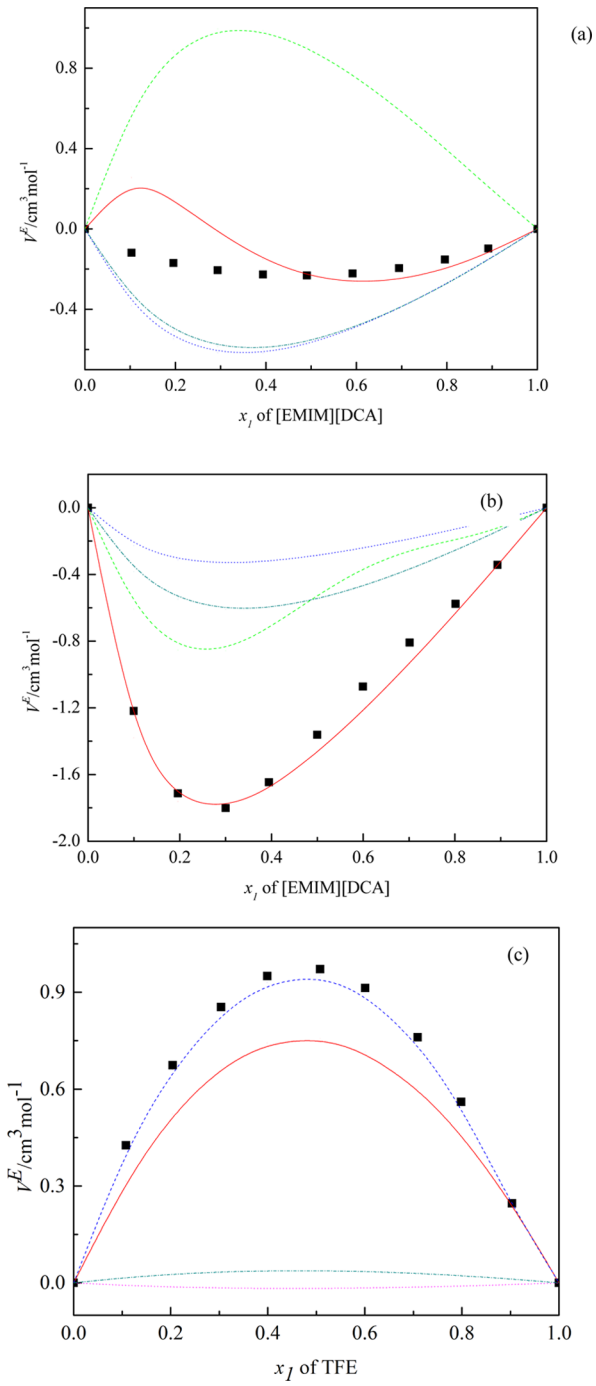

Figure 6. Experimental excess molar volumes for (a) [EMIM][DCA] + TFE, (b) [EMIM][DCA] + ethanol, and (c) TFE + ethanol binary mixtures at 298.15 K. Solid line, calculated excess molar volume from the PFP theory; dashed line, interaction contribution; dotted line, free volume contribution; and dashed−dotted line, internal pressure.

where $r(t)$ is the position of ions at a given time, $\langle \sum_{i=1}^{N} [\vec{r}_i(t) - \vec{r}_i(0)]^2 \rangle$ indicates the average of the ensemble, and D is the self-diffusion constant in cm^2/s.

As observed from Figures S19 and S20 (Supporting Information), the self-diffusion coefficient of the cation is either equal to or greater than that of the anion over the entire composition range. It is also noteworthy that the self-diffusion coefficients of the ions increase with an increase in the cosolvent concentration in the mixture. As from the RDFs, the increase of "D" is associated with a weakening of the electrostatic interactions between the ions. Moreover, the increase in the self-diffusion coefficient is more pronounced in the case of the cation [EMIM]$^+$. Once again, this is primarily due to the fact that the cosolvent associates more strongly with the anion than with the cation of IL. Our results are consistent with the reported effect of cosolvent concentration on the self-diffusion coefficient by Osti et al.[50] who reported in a study with various cosolvents and [BMIM][NTf$_2$] mixture that solvents with higher dipole moment could induce higher mobility of ions. The authors showed that with the addition of solvents such as methanol (dipole moment = 2.87 D) and acetonitrile (dipole moment = 3.92 D), the ionic self-diffusion coefficients increased by a factor of 100 until 0.40 mass fraction of [BMIM][NTf$_2$] was added to the system, similar to what we see here with the addition of TFE (dipole moment = 2.50 D), as seen in Figure S19 (Supporting Information). Furthermore, the authors also found that the molecular weight of solvents also had a strong relationship with the diffusivity of ILs along with the dipole moments. The reported study showed that solvents such as propylene carbonate and dimethyl sulfoxide have dipole moments of 4.94 and 3.96 D, respectively, which are higher than those of acetonitrile and methanol, but they induce a lower self-diffusion constant in ILs as compared to acetonitrile and methanol that are much lighter in molecular weight. TFE is a unique molecule given that it is much more heavier than acetonitrile (41.05 g/mol) and methanol (32.04 g/mol) with a molecular weight of 100.04 g/mol, similar to the molecular weight of propylene carbonate (102.09 g/mol), yet it can induce such high movement of ions in mixtures in spite of its lower dipole moment as compared with methanol, acetonitrile, propylene carbonate, and dimethyl sulfoxide. A similar finding is observed regarding the self-diffusion coefficients of ions in the [EMIM][DCA] + ethanol mixture. Our results show that quantitatively the self-diffusion constants of the cation and anion are slightly higher in ethanol as compared to TFE at both studied temperatures which follows the correlation mentioned above; ethanol is lighter in terms of molecular weight but possesses a higher dipole moment compared to TFE. Osti et al.[50] also reported that the self-diffusion constant of [BMIM][NTf$_2$] decreases with increasing alkyl chain length of alcohols. Interestingly, the self-diffusion coefficient of the cation is nearly identical to that of the anion in ethanol. As expected, the self-diffusion coefficients are enhanced with increasing temperature in both systems. Figures S19 and S20 (Supporting Information) also depict the inverse of viscosity as a function of IL concentration, which shows that the inverse of viscosity and self-diffusion coefficients exhibit similar behavior with the concentration of ILs.

Recently, based on the dissipation of stress time−correlation function and that of the time-dependent structure factors, Yamaguchi showed that the viscosity of the ILs 1-ethyl-3-methylimidazolium bis(trifluoromethylsulfonyl)imide [EMIM][NTf$_2$] and 1-octyl-3-methyl-imidazolium bis-(trifluoromethylsulfonyl)imide [OMIM][NTf$_2$] is related to the decorrelation time associated with the decay of the intermediate peak in the respective structural factors.[51] Expanding on this idea, Margulis and co-workers[52] demonstrated that the time constant associated with the dissipation of the partial structure factor for the cation head−anion at the charge alternation peak is very similar to the time scale for the decay of the stress tensor Green−Kubo correlation function, from which viscosity can be calculated. The authors concluded

https://dx.doi.org/10.1021/acs.jced.0c00447
J. Chem. Eng. Data XXXX, XXX, XXX−XXX

that this phenomenon is linked to charge blurring, that is, although the charge network persists, the ions have moved randomly so that the charge network has lost the memory of its original location. For alcohols such as methanol, Yamaguchi and Faraone[53] suggested that the shear viscosity of methanol is affected by the dynamics of the hydrogen bonding network. Based on these investigations, it is possible that the reduction in the viscosity of the IL upon addition of ethanol or TFE could be associated with a lowering in the timescale for the reorganization of the polar network of the IL in solution in comparison to that for the pure IL. From the perspective of the pure alcohol, the IL addition leads to an increase in the viscosity of the solution. Therefore, it is also plausible that the dynamics of the hydrogen-bonding network of the alcohols is retarded. Although these are intriguing possibilities, we defer the related investigation to a future study as the primary objective of the MD effort in this work is on elucidating the structural changes in [EMIM][DCA] in the presence of ethanol and TFE.

3.3.2. Radial Distribution Functions. In order to obtain molecular-level insights into the interaction between the IL and cosolvents, structural analysis in terms of RDFs is carried out and plotted using GROMACS. Figure S21 (Supporting Information) represents the distribution of hydroxyl hydrogen of TFE with the terminal nitrogen atom of $[DCA]^-$ for the [EMIM][DCA] + TFE mixture simulated in this work. The intensity of the first peak in these RDFs is quite strong, reaching ∼23 for the highest TFE concentration. With increasing IL concentration, there is a reduction in the intensity, but even at 0.9 mol fraction of the IL, the first peak in this RDF approaches ∼14. For all the concentrations, the location of the first peak is close to 1.73 Å. This can also be visualized with the coordination plot in Figure S22 (Supporting Information). The number of terminal hydrogen atoms around the terminal nitrogen atom increases steadily until 1.73 Å after which it stays close to constant until the next coordination shell. The proximity of the H atom in TFE to the N atom in $[DCA]^-$ combined with the intensity and sharpness of the first peak points to extremely favorable hydrogen bonding due to the addition of TFE. On the other hand, mixtures of [EMIM][DCA] + ethanol are marked by the absence of such a strong first peak intensity as observed in Figure S23 (Supporting Information) at any of the ethanol concentrations. Additionally, the location of the first peak is around 1.83 Å, which is slightly farther away compared to the peak of the [EMIM][DCA] + TFE mixture. This can be visualized with the coordination plot in Figure S24 (Supporting Information). The presence of strong hydrogen bonding between TFE and ILs such as $[BMIM][NTf_2]$ has also been reported by Brennecke et al.[54] at 0.65 mol fraction of TFE. It is interesting to observe that this is precisely the TFE concentration at which the intensity of the first peak drops from ∼24 to ∼17, as seen in Figure S21 of the Supporting Information. The decrease in the peak intensity also coincides with the sudden change in the self-diffusion coefficient, as suggested in Figures S19 and S20 (Supporting Information). It is conceivable that, at this IL concentration and above, the larger size of the cation prevents TFE from interacting with $[DCA]^-$. This is exacerbated by the fact that there are not enough TFE molecules to participate in hydrogen bonding with $[DCA]^-$ anions.

Trivedi et al.[55] observed similar behavior with the addition of TFE as a cosolvent in $[BMIM][PF_6]$ suggesting "hyperpolarity," meaning that the polarity of the mixture is higher than that of either of the pure components. To explain the findings, the dominant interaction between solvent−anion is invoked. A recent report in the literature[53] on the study of TFE and $[BMIM][NTf_2]$ also demonstrated hyperpolarity for these mixtures based on solvatochromic studies. The authors also conducted MD simulations to identify the interactions between various components in the mixtures. The center of mass (com) RDF analysis revealed that TFE associates strongly with the anion, consistent with our findings, and because of its acidic nature, TFE shows similar strong hydrogen-bonding interactions even with common solvents such as ethanol as reported by ref 56 and the results obtained in this study, but when mixed with ILs, these interactions tend to be extremely strong and unique. In all studies with ILs, such intense polarity is usually attributed to strong hydrogen-bonding interactions, but there could be many other forces and interactions causing this "hyperpolarity." Detailed quantum calculations could shed light on this unique behavior between TFE and ILs.

4. CONCLUSIONS

The V^E of the studied binary mixtures of IL with TFE/ethanol are found to be negative in the whole range of concentrations at all the focused temperatures with minima at $x_1 = 0.5$ for IL + TFE and at $x_1 = 0.3$ for the IL + ethanol system. The value becomes more negative with the increase of temperature from 298.15 to 323.15 K for both the binary mixtures, IL + TFE/ethanol. However, for the TFE + ethanol system, the values of V^E are found to be positive over the entire mole fraction range at all temperatures (298.15−323.15 K) with minima at $x_1 = 0.9$. With the increase of temperature from 298.15 to 323.15 K, the V^E becomes more positive. The negative deviation from ideality suggests the existence of a stronger attractive interaction in the mixture than in the pure components, and it elucidates the fact that the attractive interaction occurred owing to the accommodation of molecules of one component into the interstitial sites of the structural network of the other component. Moreover, it is also contributed by the interaction between unlike molecules through the formation of H-bonds or charge-transfer complexes or any other nonspecific forces (ion−dipole interactions, etc.) which resulted in the contraction of volume. Furthermore, the negative deviation also reveals that the system has a stronger packing efficiency by heteroassociation between the molecules of ILs and solvents via other nonspecific forces. Whereas the positive values of V^E is ascribed to the weaker association between the molecules of TFE and ethanol via H-bonding. The values of ΔK_s of the [EMIM][DCA] + TFE/ethanol systems are found to be negative throughout the composition range at all the temperatures under atmospheric pressure, while for the TFE + ethanol system, the values of ΔK_s are found to be positive over the entire mole fraction range. Its magnitude decreased and became more negative with the rise of temperature for the binary mixtures [EMIM][DCA] + TFE and [EMIM][DCA] + ethanol. Furthermore, for the TFE + ethanol system, the value increased with temperature. The ΔK_s data explain the compressibility nature of the system, and herein, both the systems are less compressible than the ideal one attributing the strong interaction between the molecules of IL and solvent. On the other hand, $\Delta\eta$ is dependent on the shape and size of the molecules and the specific molecular interaction. The $\Delta\eta$ has also been found to be negative for the [EMIM][DCA] + TFE,

https://dx.doi.org/10.1021/acs.jced.0c00447
J. Chem. Eng. Data XXXX, XXX, XXX−XXX

[EMIM][DCA] + ethanol, and TFE + ethanol systems and the values increase with an increase in temperature, but for the, TFE + ethanol system, $\Delta\eta$ are found to be negative but comparatively of lesser magnitude at all the studied compositions and temperatures and increase with an increase in temperature. The $\Delta\eta$ is attributed to the specific shape and size of the molecule and their molecular interactions. The negative deviation suggests the existence of stronger interactions, while the positive deviation suggests the weaker one between the IL and solvent molecules. The sign and magnitude of excess/deviation properties illustrate the effect of composition and temperature on the interactions in the studied binary systems. The V^E, ΔK_s and $\Delta\eta$ for each binary mixture have been fitted to the Redlich−Kister polynomial equation.

The PFP theory has been applied to correlate the excess molar volumes of [EMIM][DCA] + TFE/ethanol and TFE + ethanol binary mixtures. The PFP theory is found to be suitable for correlating the V^E of [EMIM][DCA] + TFE/ethanol and TFE + ethanol systems.

MD simulations are employed to complement the experimental results and provide an insight into the molecular interactions for the mixtures. The densities obtained from simulations are in excellent agreement with the experimental data throughout the entire composition for the studied systems. As for the excess molar volume, our simulation study is able to capture the sign of the excess molar volume correctly, while the magnitude deviated considerably. The RDF plot between the hydrogen bonding sites of the cation and TFE showed the presence of highly strong IL−solute molecular interactions for [EMIM][DCA] + TFE while slightly lower for the [EMIM][DCA] + ethanol mixture. The self-diffusion constant values depicted the occurrence of enhanced ion movements as more TFE was added to the system. This insight could help in the selection of design solvents to be mixed with ILs that could be applicable in various electrochemical applications of ILs in batteries and fuel cells.

■ ASSOCIATED CONTENT

Supporting Information

The Supporting Information is available free of charge at https://pubs.acs.org/doi/10.1021/acs.jced.0c00447.

Comparison of experimental and literature data along with PDs; values of simulated densities; measured data for the density, speed of sound, and viscosity; calculated excess molar volume via MD simulation; calculated values of excess molar volumes, excess molar isentropic compressibilities, and viscosity deviations for binary/ternary systems; chemical structures of species; snapshot of the simulation box for [EMIM][DCA]; snapshots of solvent (TFE) and anion [DCA], solvent (TFE) and cation [EMIM], and anion [DCA] and cation [EMIM] interactions around TFE; snapshots of solvent (ethanol) and anion [DCA], solvent (ethanol) and cation [EMIM], and anion [DCA] and cation [EMIM] interactions around ethanol; plots of simulation versus experimental density and experimental excess molar volume; plots of mean square displacements; graph of self-diffusion constants; plots of RDF; coordination number details; plots of equilibrated density and equilibrated total energy of systems; intensive Coulombic electrostatic interactions; and calculations of atom numbering (PDF)

■ AUTHOR INFORMATION

Corresponding Authors

Riyazuddeen − *Department of Chemistry, Aligarh Muslim University, Aligarh 202002, U.P., India;* orcid.org/0000-0002-2745-0592; Email: rz1@rediffmail.com

Jindal K. Shah − *School of Chemical Engineering, Oklahoma State University, Stillwater 74078, Oklahoma, United States;* orcid.org/0000-0002-3838-6266; Email: jindal.shah@okstate.edu

Authors

Urooj Fatima − *Department of Chemistry, Aligarh Muslim University, Aligarh 202002, U.P., India*

Pratik Dhakal − *School of Chemical Engineering, Oklahoma State University, Stillwater 74078, Oklahoma, United States*

Complete contact information is available at: https://pubs.acs.org/10.1021/acs.jced.0c00447

Notes

The authors declare no competing financial interest.

■ ACKNOWLEDGMENTS

The authors (Riyazuddeen and U.F.) are thankful to the Chairman, Department of Chemistry, A.M.U., Aligarh, for providing the necessary facility for compilation of this work. Financial support from the UGC-M.R.P. [F. no. 41−240/2012(SR)], UGC-SAP-DRS II, DST-FIST, and DST- PURSE Programs is sincerely acknowledged.

■ REFERENCES

(1) Nelyubina, Y. V.; Shaplov, A. S.; Lozinskaya, E. I.; Buzin, M. I.; Vygodskii, Y. S. A New Volume-Based Approach for Predicting Thermophysical Behavior of Ionic Liquids and Ionic Liquid Crystals. *J. Am. Chem. Soc.* **2016**, *138*, 10076−10079.

(2) Emel'yanenko, V. N.; Verevkin, S. P.; Heintz, A. The Gaseous Enthalpy of Formation of the Ionic Liquid 1-Butyl-3- Methylimidazolium Dicyanamide from Combustion Calorimetry, Vapor Pressure Measurements, and Ab Initio Calculations. *J. Am. Chem. Soc.* **2007**, *129*, 3930−3937.

(3) Méndez-Morales, T.; Carrete, J.; Cabeza, O.; Gallego, L. J.; Varela, L. M. Molecular Dynamics Simulations of the Structural and Thermodynamic Properties of Imidazolium-Based Ionic Liquid Mixtures. *J. Phys. Chem. B* **2011**, *115*, 11170−11182.

(4) Bhanuprakash, P.; Narasimha Rao, C.; Sivakumar, K. Evaluation of Molecular Interactions by Volumetric and Acoustic Studies in Binary Mixtures of the Ionic Liquid [EMIM][MeSO4] with Ethanoic and Propanoic Acid at Different Temperatures. *J. Mol. Liq.* **2016**, *219*, 79−87.

(5) Li, Y.; Figueiredo, E. J. P.; Santos, M. J.; Santos, J. B.; Talavera-Prieto, N. M. C.; Carvalho, P. J.; Ferreira, A. G. M.; Mattedi, S. Volumetric and Acoustical Properties of Aqueous Mixtures of N-Methyl-2-Hydroxyethylammonium Butyrate and N-Methyl-2-Hydroxyethylammonium Pentanoate at T = (298.15 to 333.15) K. *J. Chem. Thermodyn.* **2016**, *97*, 191−205.

(6) Fernández, A.; Torrecilla, J. S.; García, J.; Rodríguez, F. Thermophysical Properties of 1-Ethyl-3-Methylimidazolium Ethylsulfate and 1-Butyl-3-Methylimidazolium Methylsulfate Ionic Liquids. *J. Chem. Eng. Data* **2007**, *52*, 1979−1983.

(7) Yao, H.; Zhang, S.; Wang, J.; Zhou, Q.; Dong, H.; Zhang, X. Densities and Viscosities of the Binary Mixtures of 1-Ethyl-3-methylimidazolium Bis(trifluoromethylsulfonyl)imide with N-Meth-

yl-2-pyrrolidone or Ethanol at T = (293.15 to 323.15) K. *J. Chem. Eng. Data* **2012**, *57*, 875−881.

(8) Han, S.; Li, J.; Zhu, S.; Chen, R.; Wu, Y.; Zhang, X. *Cellulose Derivatives: Synthesis, Structure, and Properties*; Springer, 2009.

(9) Govinda, V.; Attri, P.; Venkatesu, P.; Venkateswarlu, P. Evaluation of Thermophysical Properties of Ionic Liquids with Polar Solvent: A Comparable Study of Two Families of Ionic Liquids with Various Ions. *J. Phys. Chem. B* **2013**, *117*, 12535−12548.

(10) Sharma, V. K.; Solanki, S.; Bhagour, S. Thermodynamic Properties of Ternary Mixtures Containing Ionic Liquid and Organic Liquids: Excess Molar Volume and Excess Isentropic Compressibility. *J. Chem. Eng. Data* **2014**, *59*, 1140−1157.

(11) Kowsari, M. H.; Tohidifar, L. Tracing Dynamics, Self-Diffusion, and Nanoscale Structural Heterogeneity of Pure and Binary Mixtures of Ionic Liquid 1-Hexyl-2,3-Dimethylimidazolium Bis-(Fluorosulfonyl)Imide with Acetonitrile: Insights from Molecular Dynamics Simulations. *J. Phys. Chem. B* **2016**, *120*, 10824−10838.

(12) Liu, J.; Chambreau, S. D.; Vaghjiani, G. L. Dynamics Simulations and Statistical Modeling of Thermal Decomposition of 1-Ethyl-3-Methylimidazolium Dicyanamide and 1-Ethyl-2,3-Dimethylimidazolium Dicyanamide. *J. Phys. Chem. A* **2014**, *118*, 11133−11144.

(13) Tomaz, M. M. F.; França, J. M. P.; Viera, S. I. C.; Sohel Murshed, S. M.; Lourenço, M. J. V. *Thermophysical Properties of [C2mim][CH3SO3] - Experimental and Heat Transfer Studies*, 2013, No. 2009, 2575.

(14) Anwar, N.; Riyazuddeen. Interaction of 1-Butyl-3-methylimidazolium Trifluoromethanesulfonate with Ethyl Acetate/1-Butanol: Thermophysical Properties. *J. Solution Chem.* **2016**, *45*, 1077−1094.

(15) Fatima, U.; Riyazuddeen; Anwar, N. Effect of Solvents and Temperature on Interactions in Binary and Ternary Mixtures of 1-Butyl-3-Methylimidazolium Trifluoromethanesulfonate with Acetonitrile or/and N, N-Dimethylformamide. *J. Chem. Eng. Data* **2018**, *63*, 4288−4305.

(16) Fatima, U.; Riyazuddeen; Anwar, N.; Montes-Campos, H.; Varela, L. M. Molecular Dynamic Simulation, Molecular Interactions and Structural Properties of 1-Butyl-3-Methylimidazolium Bis-(Trifluoromethylsulfonyl)Imide + 1-Butanol/1-Propanol Mixtures at (298.15−323.15) K and 0.1 M Pa. *Fluid Phase Equilib.* **2018**, *472*, 9−21.

(17) Vataščin, E.; Dohnal, V. Thermodynamic Properties of Aqueous Solutions of [EMIM] Thiocyanate and [EMIM] Dicyanamide. *J. Chem. Thermodyn.* **2017**, *106*, 262−275.

(18) Quijada-Maldonado, E.; Van Der Boogaart, S.; Lijbers, J. H.; Meindersma, G. W.; De Haan, A. B. Experimental Densities, Dynamic Viscosities and Surface Tensions of the Ionic Liquids Series 1-Ethyl-3-Methylimidazolium Acetate and Dicyanamide and Their Binary and Ternary Mixtures with Water and Ethanol at T = (298.15 to 343.15 K). *J. Chem. Thermodyn.* **2012**, *51*, 51−58.

(19) Schreiner, C.; Zugmann, S.; Hartl, R.; Gores, H. J. Fractional Walden Rule for Ionic Liquids: Examples from Recent Measurements and a Critique of the So-Called Ideal KCl Line for the Walden Plot. *J. Chem. Eng. Data* **2010**, *55*, 1784−1788.

(20) Fröba, A. P.; Kremer, H.; Leipertz, A.; Erlangen. Density, Refractive Index, Interfacial Tension, and Viscosity of Ionic Liquids [EMIM][$EtSO_4$], [EMIM][NTf_2], [EMIM][$N(CN)_2$], and [OMA]-[NTf_2] in Dependence on Temperature at Atmospheric Pressure. *J. Chem. Eng. Data* **2008**, *112*, 12420−12430.

(21) Neves, C. M. S. S.; Carvalho, P. J.; Freire, M. G.; Coutinho, J. A. P. Thermophysical Properties of Pure and Water-Saturated Tetradecyltrihexylphosphonium-Based Ionic Liquids. *J. Chem. Thermodyn.* **2011**, *43*, 948−957.

(22) Klomfar, J.; Součková, M.; Pátek, J. Temperature Dependence of the Surface Tension and Density at 0.1 MPa for 1-Ethyl- and 1-Butyl-3-Methylimidazolium Dicyanamide. *J. Chem. Eng. Data* **2011**, *56*, 3454−3462.

(23) Wong, C.-L.; Soriano, A. N.; Li, M.-H. Diffusion Coefficients and Molar Conductivities in Aqueous Solutions of 1-Ethyl-3-Methylimidazolium-Based Ionic Liquids. *Fluid Phase Equilib.* **2008**, *271*, 43−52.

(24) Nakamura, M.; Chubachi, K.; Tamura, K.; Murakami, S. Excess molar volumes, excess isentropic and isothermal compressibilities, and excess molar isochoric heat capacities of [xCF3CH2OH + (1-x){HCON(CH3)2 or CH3CN}] at the temperature 298.15 K. *J. Chem. Thermodyn.* **1993**, *25*, 525−531.

(25) Minamihonoki, T.; Ogawa, H.; Nomura, H.; Murakami, S. Thermodynamic properties of binary mixtures of 2,2,2-trifluoroethanol with water or alkanols at T=298.15K. *Thermochim. Acta* **2007**, *459*, 80−86.

(26) Riddick, J. A.; Bunger, W. B.; Sakano, T. K. *Organic Solvents: Physical Properties and Methods of Purification*; U.S. Department of Energy Office of Scientific and Technical Information, 1986.

(27) Salgado, J.; Regueira, T.; Lugo, L.; Vijande, J.; Fernández, J.; García, J. Density and viscosity of three (2,2,2-trifluoroethanol+1-butyl-3-methylimidazolium) ionic liquid binary systems. *J. Chem. Thermodyn.* **2014**, *70*, 101−110.

(28) Pérez, E.; Mainar, A. M.; Santafé, J.; Urieta, J. S. Excess Enthalpy, Excess Volume, Viscosity Deviation, and Speed of Sound Deviation for the Mixture Tetrahydropyran + 2,2,2-Trifluoroethanol at (283.15, 298.15, and 313.15) K. *J. Chem. Eng. Data* **2003**, *48*, 723−726.

(29) Esteve, X.; Patil, K. R.; Fernández, J.; Coronas, A. Prediction of Density and Excess Volume for the Ternary Mixture: (Water + 2,2,2-Trifluoroethanol + 2,5,8,11,14-Pentaoxapentadecane) from Experimental Binary Values at Temperatures from 283.15 k to 333.15 K. *J. Chem. Thermodyn.* **1995**, *27*, 281−292.

(30) Sassi, M.; Atik, Z. Excess molar volumes of binary mixtures of 2,2,2-trifluoroethanol with water, or acetone, or 1,4-difluorobenzene, or 4-fluorotoluene, or α,α,α, trifluorotoluene or 1-alcohols at a temperature of 298.15 K and pressure of 101 kPa. *J. Chem. Thermodyn.* **2003**, *35*, 1161−1169.

(31) Mukherjee, L. H.; Grunwald, E. Physical Properties and Hydrogen Bonding in the System Ethanol-2,2,2- Trifluoroethanol. *J. Phys. Chem.* **1958**, *62*, 1311−1314.

(32) Duarte, P.; Silva, M.; Rodrigues, D.; Morgado, P.; Martins, L. F. G.; Filipe, E. J. M. Liquid Mixtures Involving Hydrogenated and Fluorinated Chains: (p, ρ, T, x) Surface of (Ethanol + 2,2,2-Trifluoroethanol), Experimental and Simulation. *J. Phys. Chem. B* **2013**, *117*, 9709−9717.

(33) Sánchez, M. A.; Mainar, A. M.; Pardo, J. I.; López, M. C.; Urieta, J. S. Solubility of Nonpolar Gases in 2 , 2 , 2-Trifluoroethanol Temperatures and 101 . 33 KPa Partial Pressure of Gas. *Can. J. Chem.* **2001**, *79*, 1460−1465.

(34) Gómez, E.; González, B.; Calvar, N.; Tojo, E.; Domínguez, Á. Physical Properties of Pure 1-Ethyl-3-Methylimidazolium Ethylsulfate and Its Binary Mixtures with Ethanol and Water at Several Temperatures. *J. Chem. Eng. Data* **2006**, *51*, 2096−2102.

(35) Nikam, P. S.; Jadhav, M. C.; Hasan, M. Density and Viscosity of Mixtures of Dimethyl Sulfoxide + Methanol, +ethanol, +propan-1-Ol, +propan-2-Ol, +butan-1-Ol, +2-Methylpropan-1-Ol, and +2-Methylpropan-2-Ol at 298.15 K and 303.15 K. *J. Chem. Eng. Data* **1996**, *41*, 1028−1031.

(36) González, B.; Calvar, N.; Gómez, E.; Domínguez, Á. Density, dynamic viscosity, and derived properties of binary mixtures of methanol or ethanol with water, ethyl acetate, and methyl acetate at T=(293.15, 298.15, and 303.15)K. *J. Chem. Thermodyn.* **2007**, *39*, 1578−1588.

(37) Secondary, C. A.; Author, C.; Jose, N.; Lopes, C. Modeling Ionic Liquids Using a Systematic All-Atom Force Field. *J. Phys. Chem. B* **2004**, *108*, 2038−2047.

(38) Canongia Lopes, J. N.; Pádua, A. A. H. Molecular Force Field for Ionic Liquids III: Imidazolium, Pyridinium, and Phosphonium Cations; Chloride, Bromide, and Dicyanamide Anions. *J. Phys. Chem. B* **2006**, *110*, 19586−19592.

(39) Jorgensen, W. L.; Maxwell, D. S.; Tirado-Rives, J. Development and Testing of the OPLS All-Atom Force Field on Conformational

https://dx.doi.org/10.1021/acs.jced.0c00447
J. Chem. Eng. Data XXXX, XXX, XXX−XXX

Energetics and Properties of Organic Liquids. *J. Am. Chem. Soc.* **1996**, *118*, 11225−11236.

(40) Chitra, R.; Smith, P. E. A Comparison of the Properties of 2,2,2-Trifluoroethanol and 2,2,2-Trifluoroethanol/Water Mixtures Using Different Force Fields. *J. Chem. Phys.* **2001**, *115*, 5521−5530.

(41) Hess, B.; Kutzner, C.; Van Der Spoel, D.; Lindahl, E. GROMACS 4: Algorithms for Highly Efficient, Load-Balanced, and Scalable Molecular Simulation. *J. Chem. Theory Comput.* **2008**, *4*, 435−447.

(42) Martínez, L.; Andrade, R.; Birgin, E. G.; Martínez, J. M. PACKMOL: A Package For Building Initial Configurations For Molecular Dynamics Simulations. *J. Comput. Chem.* **2009**, *30*, 2157−2164.

(43) Hoover, W. G. Canonical Dynamics: Equilibrium Phase-Space Distributions. *Am. Phys. Soc.* **1985**, *31*, 1695−1697.

(44) Parrinello, M.; Rahman, A. Polymorphic Transitions in Single Crystals: A New Molecular Dynamics Method. *J. Appl. Phys.* **1981**, *52*, 7182−7190.

(45) Yu, Y.-H.; Soriano, A. N.; Li, M.-H. Heat Capacities and Electrical Conductivities of 1-Ethyl-3-Methylimidazolium-Based Ionic Liquids. *J. Chem. Thermodyn.* **2009**, *41*, 103−108.

(46) Coronas, A.; Vallés, A.; Chaudhari, S. K.; Patil, K. R. Absorption Heat Pump with the TFE-TEGDME and TFE-H20-TEGDME Systems. *Appl. Therm. Eng.* **1996**, *16*, 335−345.

(47) Vega-Maza, D.; Segovia, J. J.; Carmen Martín, M.; Villamañán, R. M.; Villamañán, M. A. Thermodynamic Properties of Biofuels: Heat Capacities of Binary Mixtures Containing Ethanol and Hydrocarbons up to 20 MPa and the Pure Compounds Using a New Flow Calorimeter. *J. Chem. Thermodyn.* **2011**, *43*, 1893−1896.

(48) Benson, G. C.; D'Arcy, P. J. Excess Isobaric Heat Capacities of Water-n-Alcohol Mixtures. *J. Chem. Eng. Data* **1982**, *27*, 439−442.

(49) DDB. The Dortmund data bank, ionic liquids in the Dortmund data bank. http://www.ddbst.de/new/frame-ionic-liquids.htm.

(50) Osti, N. C.; Van Aken, K. L.; Thompson, M. W.; Tiet, F.; Jiang, D.-e.; Cummings, P. T.; Gogotsi, Y.; Mamontov, E. Solvent Polarity Governs Ion Interactions and Transport in a Solvated Room-Temperature Ionic Liquid. *J. Phys. Chem. Lett.* **2017**, *8*, 167−171.

(51) Yamaguchi, T. Coupling Between the Mesoscopic Dynamics and Shear Stress of a Room-Temperature Ionic Liquid. *Phys. Chem. Chem. Phys.* **2018**, *20*, 17809−17817.

(52) Amith, W. D.; Araque, J. C.; Margulis, C. J. A Pictorial View of Viscosity in Ionic Liquids and the Link to Nanostructural Heterogeneity. *J. Phys. Chem. Lett.* **2020**, *11*, 2062−2066.

(53) Yamaguchi, T.; Faraone, A. Analysis of Shear Viscosity and Viscoelastic Relaxation of Liquid Methanol Based on Molecular Dynamics Simulation and Mode-Coupling Theory. *J. Chem. Phys.* **2017**, *146*, 244506−244508.

(54) Mellein, B. R.; Aki, S. N. V. K.; Ladewski, R. L.; Brennecke, J. F. Solvatochromic Studies of Ionic Liquid/Organic Mixtures. *J. Phys. Chem. B* **2007**, *111*, 131−138.

(55) Trivedi, S.; Pandey, S.; Baker, S. N.; Baker, G. A.; Pandey, S. Pronounced Hydrogen Bonding Giving Rise to Apparent Probe Hyperpolarity in Ionic Liquid Mixtures with 2,2,2-Trifluoroethanol. *J. Phys. Chem. B* **2012**, *116*, 1360−1369.

(56) Islam, M. R.; Warsi, F.; Khan, A. B.; Kausar, T.; Khan, I.; Ali, M. Solvatochromism of Binary Mixtures of 2,2,2-Trifluoroethanol + Ionic Liquid [bmim][Tf2N]: A Comparative Study with Molecular Solvents. *J. Chem. Eng. Data* **2019**, *64*, 1140−1154.

https://dx.doi.org/10.1021/acs.jced.0c00447
J. Chem. Eng. Data XXXX, XXX, XXX−XXX